

Fig. 2. The linear current controller with (a) separate modulator and (b) nonlinear current controller as modulator

The systems using nonlinear elements (comparators) belong to the second group. The comparators determine the current error signs in the three phases feeding the motor. This way, the information about the desired configuration of the con-

verter state is provided (Fig. 2b). The controllers of the second group are universally assumed a solution which enables a better current control dynamic than the controllers of the first group (with PI controllers).

The current controller is responsible for the whole system quality [4]. It means that, the current control loop's respond time should be as short as possible in order to guarantee the high dynamic properties of the drive. In the steady state, the current error should have values close to zero. The current controller should fulfill the following requirements:

- precisely follow the command signal when the output frequency is changed (lack of the amplitude and phase error),
- quickly react to the command value changes ensuring good system dynamic,
- work with limited or constant switching frequency to guarantee the safe converter transistors operation.

## 2. The predictive current controller

The theory proposed by I. Nagy [5] and developed by A. Sikorski [6] can be used to analyze nonlinear systems. This theory enables the current vector changes prediction depending on the converter switching state. The predictive current controller uses this theory basing on the load and converter vectorial models (Fig. 3). There is an extensive variety of methods which can be defined as "predictive". If the control system uses knowledge about the behavior of the controlled object after force change, while choosing the optimal control, it can be called the predictive controller [7–9].

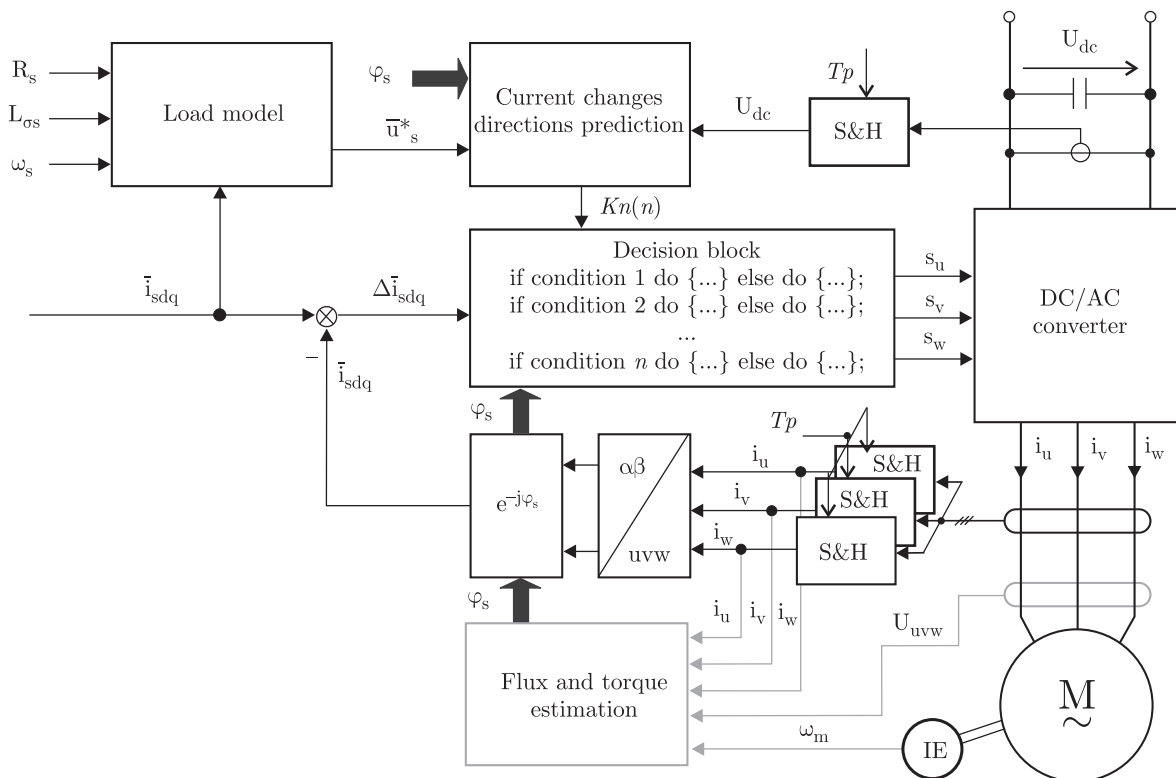


Fig. 3. The predictive current controller

Minimization current error area of the DC/AC inverter controlled by predictive current control method

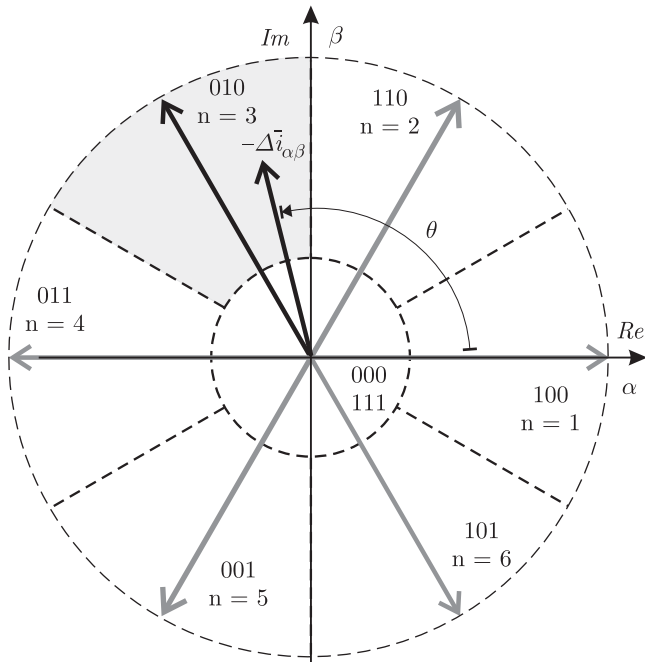


Fig. 4. The example of the complex plane division on the particular areas to which the switches configurations are described

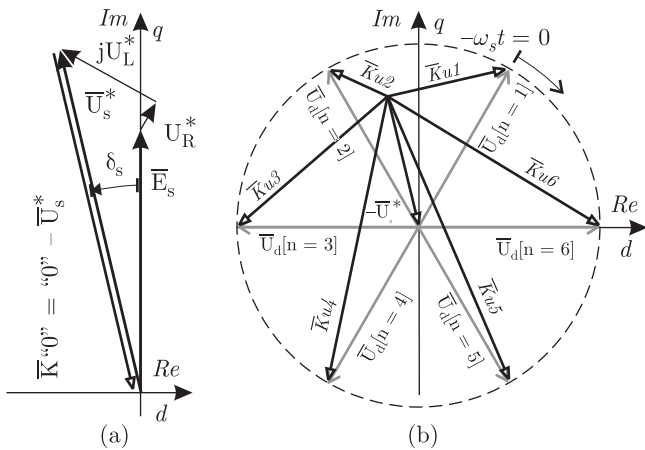


Fig. 5. The graphical illustration of the current vector move direction described by Eq. (3)

On account of the widespread application of microprocessors in control systems, predictive controllers operate with constant calculation time. It means that the decision about the converter switches states change is taken by the control system in the discrete time moments  $T_p$ . Therefore the maximal switching frequency is limited to the sampling frequency. The control system checks the error vector location on the complex plane in the discrete moments (Fig. 4). The converter transistors states are chosen depending on the vector location.

The method of mean switching frequency minimization proposed in [10] is realized by the middle of circular error area (in which the “zero” vector is used) determination. It is the consequence of the assumption that, the “zero” vector always ensures the lowest dynamic of the current changes. This assumption is true only for the low motor speed (low value

of electromotive force). With the high motor speed, close to the nominal value, the “zero” voltage vector produces the high changes of the current vector, which is the reason of the worse quality of current shaping. Therefore, the internal area (radius), in which the vector causing the slowest current changes, should be changed. It should also be checked whether it is still the “zero” vector [11,12].

3. The current vector changes prediction

The possibility of defining the current vector predicted directions’ changes forms the basis for carrying out the analysis connected with the error area minimization in the system with the predictive current controller.

Taking into equation, the converter description in  $dq$  reference frame:

$$\bar{U}_d[n] = \begin{cases} \frac{2}{3}U_{DC} \cdot e^{j[(n-1)\frac{\pi}{3} - \omega_s t]} & \text{for } n = \langle 1, 2, 3, 4, 5, 6 \rangle \\ 0 & \text{for } n = \langle 0, 7 \rangle \end{cases} \quad (1)$$

where:

$\frac{2}{3}U_{DC} \cdot e^{j[(n-1)\frac{\pi}{3} - \omega_s t]}$  – the converter output voltage vector defined by the conduction switches configuration ( $n = 1, 2, 3, 4, 5, 6$ ),  $\omega_s t$  – the synchronous angle of the vector rotation, and stator motor voltage equation for the command values:

$$\bar{U}_s^* = \bar{E}_s + R_s \bar{i}_{sdq}^* + j\omega_s L_{\sigma s} \bar{i}_{sdq}^* = U_d^* + jU_q^* \quad (2)$$

where:

$\bar{i}_{sdq}^*$  – the stator current vector command value in the rotated reference frame  $dq$ ,  
 $\bar{E}_s$  – the electromotive force vector,  
 $R_s, L_{\sigma s}$  – resistance and leakage inductance of the stator winding.

The equation describing the direction and the speed of the converter output current vector changes can be determined [12]:

$$L_{\sigma s} \frac{d}{dt} \bar{i}_{sdq}[n] = -\bar{U}_s^* + \bar{U}_d[n] = \bar{K}u[n] \quad (3a)$$

$$\frac{d}{dt} \bar{i}_{sdq}[n] = (-\bar{U}_s^* + \bar{U}_d[n]) / L_{\sigma s} = \bar{K}i[n] \quad (3b)$$

The solution of Eq. (3) depends on the parameter value  $n$  (configuration of the converter conduction switches). The graphical illustration of the current vector move direction was shown in Fig. 5. The vector  $\bar{K}u[n]$  length is determined the current vector changes speed.

Because the predictive controller operates as discrete system, the prediction of the new current vector location is made on the basis of the current vector actual location  $\bar{i}_{sdq}[p]$  (step  $p$ ) and its change induced by its derivative calculated after time  $T_p$ .

$$\bar{i}_{sdq}[p + 1] = \bar{i}_{sdq}[p] + \frac{d}{dt} \bar{i}_{sdq}[n] \cdot T_p \quad (4)$$

where:

$[p], [p + 1]$  – the following sample steps of the microprocessors system,

$[n]$  – the derivative coefficient depending on the converter conduction switches configuration ( $n = 0, 1, 2, 3, 4, 5, 6, 7$ ).

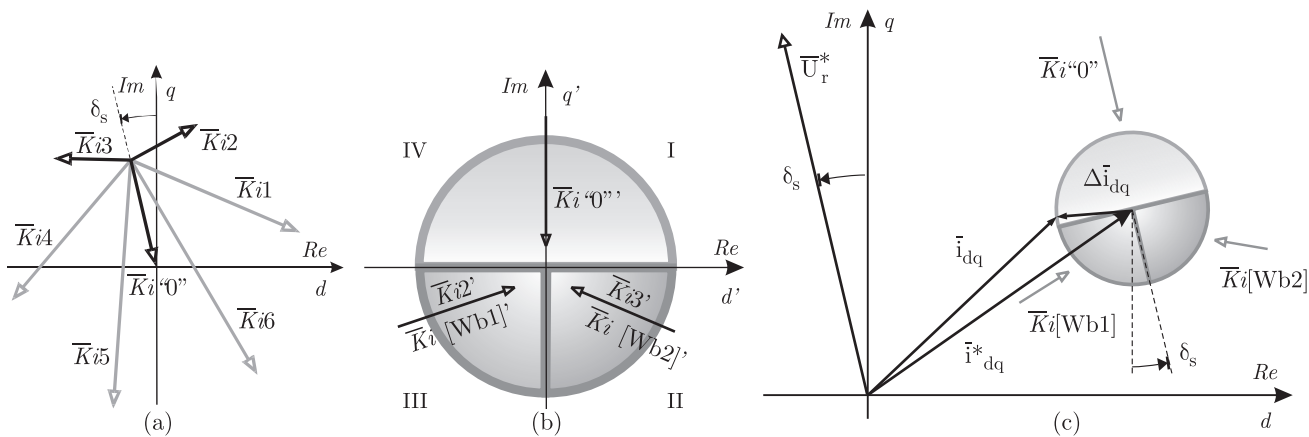


Fig. 6. The three direction vectors ensuring (a) the current vector control principle of the error area division on (b) the areas of direction vectors  $\bar{K}i[n]$  and principle of direction vectors influence on (c) the real current vector  $\bar{i}_{dq}$  for DC/AC converter

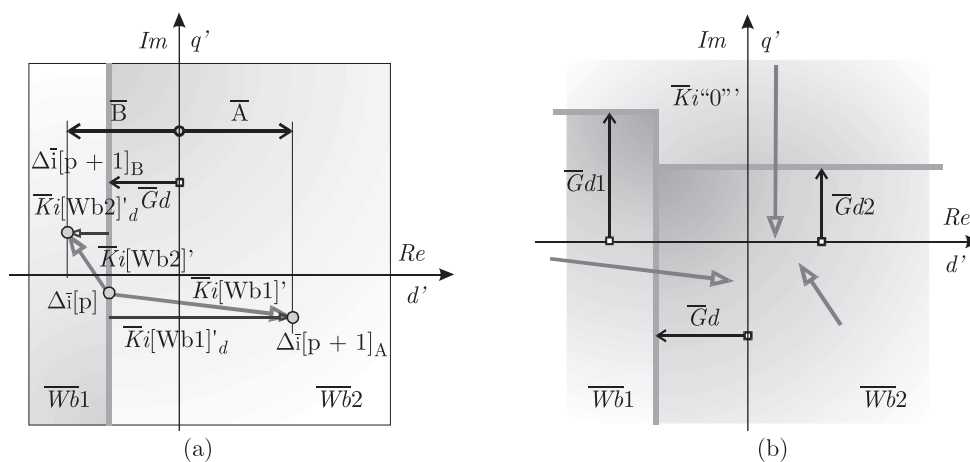


Fig. 7. The error vector  $\Delta\bar{i}[p]$  area border division move with vector (a)  $\bar{G}d$  for the two analyzed vectors  $\bar{K}i[n]$  and (b) the borders division move for the all analyzed directions vectors pairs  $\bar{K}i[n]$

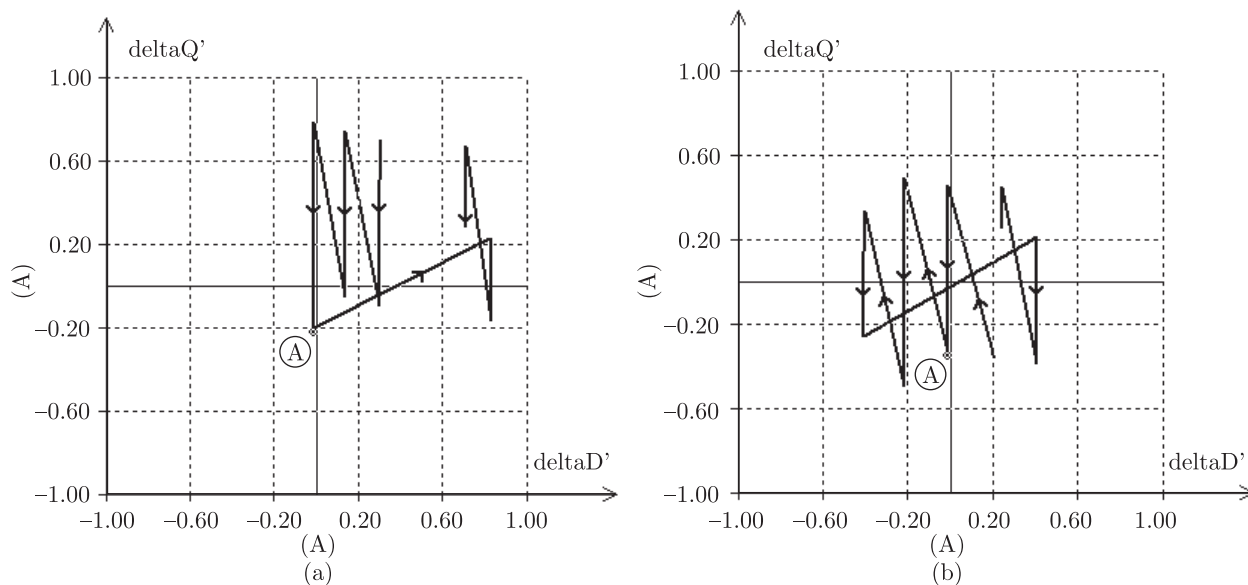


Fig. 8. The current error vector  $\Delta\bar{i}_{sdq}$  move with standard error area division (a) and with the area division border change (b) for DC/AC converter

Minimization current error area of the DC/AC inverter controlled by predictive current control method

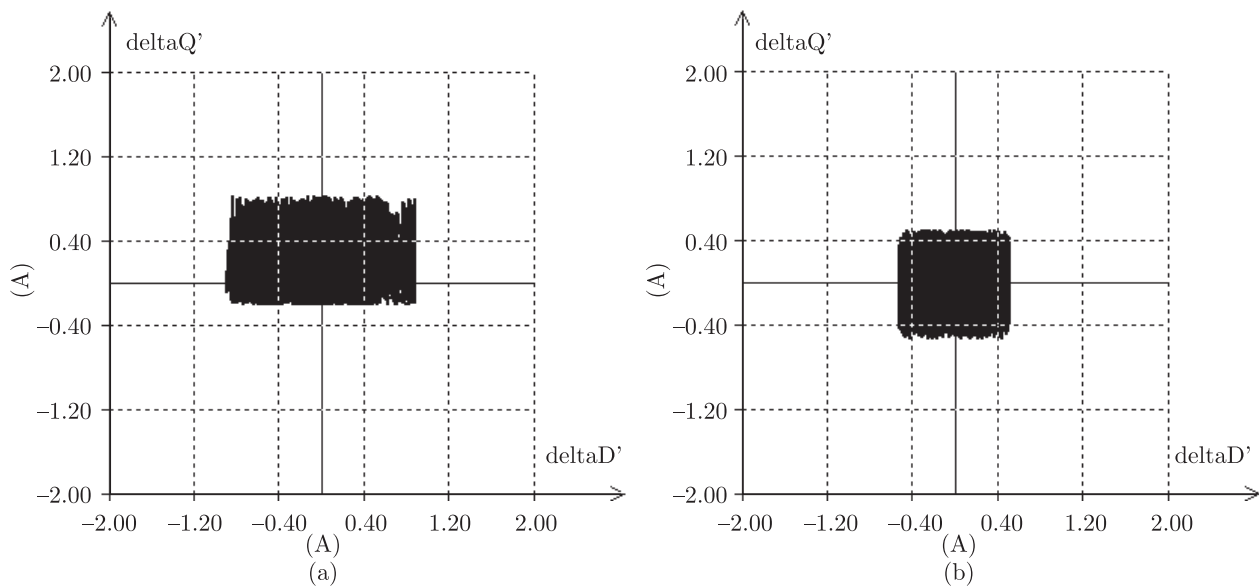


Fig. 9. The current error vector  $\Delta \bar{i}_{sdq}$  trajectory with standard error area division (a) and with the area division border change (b) for DC/AC converter

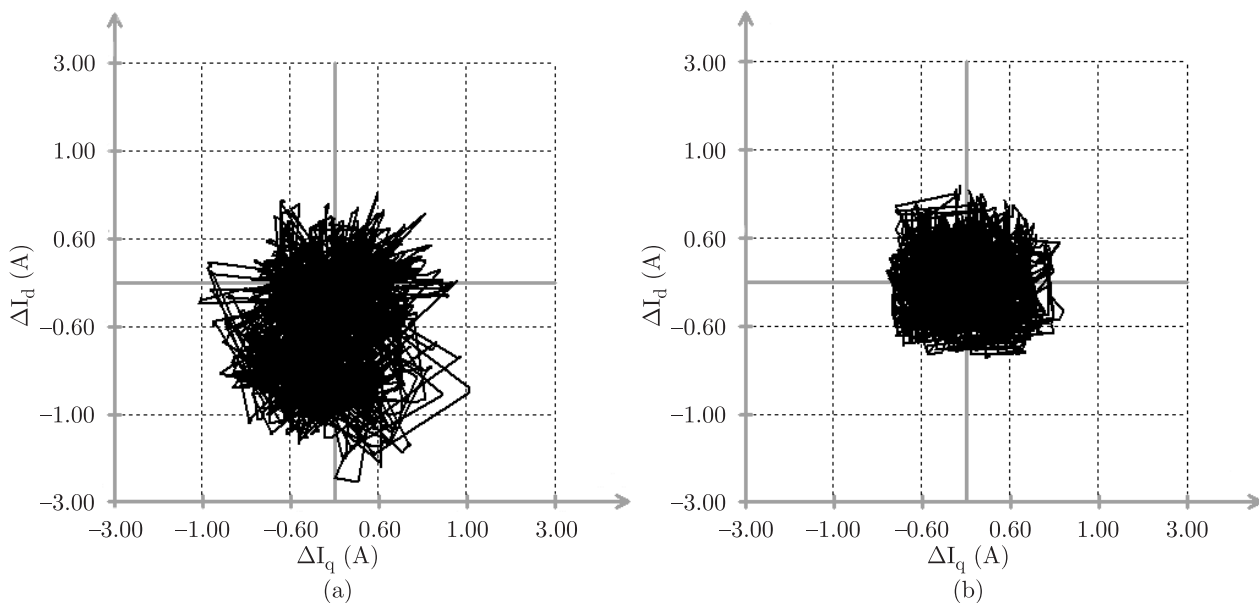


Fig. 10. The current error vector  $\Delta \bar{i}_{sdq}$  trajectory of the DC/AC converter with (a) delta-modulation current controller and with (b) predictive controller with error area division border move

It gives the possibility of the predictive current vector error  $\Delta \bar{i}_{sdq}[p+1]$  determination as well as the assessment of the correctness transistors configuration chosen (taking into account the optimization criteria).

$$\Delta \bar{i}_{sdq}[p+1] = \bar{i}_{sdq}[p+1] - \bar{i}_{sdq}^* \quad (5)$$

By analyzing the position of the vector directions  $\bar{K}u[n]$  in Fig. 5b, we can see that only three vectors  $\bar{K}u[n]$  are needed to control the output current vector. In Fig. 5b these are  $\bar{K}u[1]$ ,  $\bar{K}u[2]$  and  $\bar{K}u[0]$  vectors. The shortest direction vectors (the smaller derivative value) guarantee the smallest speed of the current changes.

#### 4. The error area minimization principle

The assumption that among from all the converter switches configurations there are three, which practically always permit to control the converter current output control (Fig. 6a) is based upon the algorithms syntheses (operating on the principle of the current vector error area division). This assumption determines the complex plane division for the three areas (Fig. 6b) to which the three output voltage vectors are described (one to each area). The output voltage vectors described to their particular areas cause the move of the error current vector into the reference frame beginning (real current vector into its com-

mand value). By checking in which sector the current error vector is, the control system chooses the switching configuration described to this area.

In order to minimize the current error vector amplitude, the vector characterized by minimal derivative should be used in the maximal part of error area, first of all, when the real current vector is close to its command value. This condition can be fulfilled by shifting the borderlines of the error area defined in Fig. 6b. The error area borderline should be moved in such direction and with such value (for example with vector  $\bar{G}d$  – Fig. 7a) so that the impact of one of the possible direction vectors ( $\bar{K}i[Wb1]'$  or  $\bar{K}i[Wb2]'$ ) on the error vector  $\Delta\bar{i}[p]$  provoked the error vector's move to one of the two feasible points ( $\Delta\bar{i}[p+1]_A$  or  $\Delta\bar{i}[p+1]_B$ ) which are equidistant to the  $q'$  axis ( $\bar{A} + \bar{B} = 0$ ). The move vector is calculated on the basis of the analysis of the competitive direction vectors ( $\bar{K}i[Wb1]'$  or  $\bar{K}i[Wb2]'$ ) influence on the length of the error component, perpendicular to the reference frame axis along which the borderline runs [13].

A separate analysis of mutual influence of the three pairs of competitive direction vectors  $\bar{K}u[n]$  allows to calculate the shift values of all borderlines of the error area. Exemplary solution to a specific system state is shown in Fig. 7b.

The initial confirmation of the analysis correctness and the error area minimization effectiveness were carried out by simulations. The comparison of the current controller without the modification of the error area borderlines as well as the current controller with the proposed modification, were carried out in the simulations. Fig. 8a shows that when current error vector  $\Delta\bar{i}_{sdq}$  takes the point "A", the second direction vector  $\bar{K}i[n]$  immediately "throws it out" to a considerable distance. The error area borderline shift definitely improves the current shaping. Fig. 8b shown a situation where current error vector takes "A" point and the long direction vector was not used.

## 5. The laboratory test results

The laboratory tests were carried out in the drive system with the following motor dates: the nominal power  $P_n = 3$  [kW], the nominal rotation  $n_n = 1415$  [ $\text{min}^{-1}$ ], the pole number  $p = 2$ , the nominal current  $I_n = 6.9$  [A], the stator nominal leakage inductance  $L_{\sigma s} = 11$  [mH] and rotor resistance  $R_s = 1.9$  [ $\Omega$ ]. The standard transistors module PM15RSH120 was used as a DC/AC converter. The control system was realized on a floating-point processor ADSP-21061. The FOC method of motor control with the current controller was applied. In the first of the examined events the delta-modulation current controller was used. In the second event, the predictive controller operating according to the principle of the error area minimization presented in this paper. The current error vector magnitude reduction is clearly presented in the figure below (Fig. 9).

About 45% of the current error vector's amplitude minimization was achieved after application of the proposed method of control. As a result, the coefficient  $THD_I = 17\%$  with delta-modulation decreased to 10% when the predictive controller was used.

Additionally the mean switching frequency with predictive controller was reduced. The switching frequency decrease results from the fact that during several sampling steps, the current error vector stays in the same error area. The same vector of converter output voltage is used. The mean switching frequency of the converter with predictive controller is 14% smaller for the nominal motor speed (about 1450 r.p.m.) than with the delta-modulation controller. In the scope of low motor velocities  $\omega_m/\omega_{nM} = 0.02$  (30 r.p.m.) the mean switching frequency is even 95% smaller (Fig. 10).

## 6. Conclusions

Results of the predictive current controller operation were compared to the system operation with delta-modulation controller. It was proved that the current error area shaped by the converter transistor can be decreased with the additional limitation of the mean switching frequency. The smaller error area means the current feeding motor ripples decrease (smaller  $THD_I$ ). The mean switching frequency decrease means the converter transistors switching power dissipation decrease (higher efficiency). The proposed method can be applied in a tabular form. The values of the error area border moves can be presented in the form of a table. The table argument is synchronous turn angle  $\omega_s t$  and the range of angular motor speed. It enables an increase of sample frequency or the system realization using slower microprocessors.

**Acknowledgements.** This work was supported by the Polish Ministry of Science and Informatization under Grant KBN 4 T10A 070 25 and Technical University of Bialystok under project W/WE/11/03.

## REFERENCES

- [1] K.B. Bose, "Power electronics and variable frequency drives: technology and applications", *Piscataway IEEE Press*, 590–592 (1997).
- [2] M.P. Kaźmierkowski, R Krishan., and F. Blaabjerg, *Control in Power Electronics – Selected Problems*, Amsterdam: Academic Press, 2002.
- [3] J. Holtz; "Pulsewidth modulation - a survey", *IEEE Transactions on Industrial Electronics* 39 (5), 410–420 (1992).
- [4] M.P. Kaźmierkowski, "Control strategies for PWM rectifier/inverter – fed induction motors", *9th Int. Conf. on Power Electronics and Motion Control, EPE-PEMC'2000* 1, 69–78 (2000).
- [5] I. Nagy, "Control algorithm of a three phase voltage sourced reversible rectifier", *4th Eur. Conf. on Power Electronics and Application* 3, Firenze, Italy, 287–292 (1991).
- [6] A. Sikorski, "Problems connected with the minimization of switching losses in AC/DC/AC - PWM converter feeding the induction machine", *Scientific Debates* 58, Technical University of Bialystok Press, Białystok, 1998, (in Polish).
- [7] J. Holtz and S. Stadtfeld, "A predictive controller for the stator current vector of AC-machines fed from a switched voltage source", *Conf. Record IPEC Tokyo* 2, 1665–1675 (1983).
- [8] J. Holtz and S. Stadtfeld, "A PWM inverter drive system with on-line optimized pulse patterns", *First Eur. Conf. on Power Electronics and Application* 3, 21–25 (1985).

*Minimization current error area of the DC/AC inverter controlled by predictive current control method*

- [9] R. Kennel and D. Schröder, "Predictive control strategy for converters", *Proc. of the Third IFAC Symposium*, Lausanne, 415–422 (1983).
- [10] E. Aldabas, J.L. Romeral, A. Arias, and M.R. Chekkouri, "Digital current controller with a very simple null-vector voltage strategy", *Proc. 9th Eur. Conf. on Power Electronics and Application*, EPE Association, 1–8 (2001).
- [11] A. Rusczyk and A. Sikorski, "Control of DC/AC inverter current to minimize the current error vector", *9th Int. Conf. on Power Electronics and Motion Control, EPE-PEMC'2000* 7, 174–180 (2000).
- [12] A. Sikorski and A. Rusczyk, "The control of DC/AC converter with the minimization of an area of a current vector error", *VI Symposium on on Ergoelectronics in Science and Didactics*, Kielce, 81–90 (2000), (in Polish).
- [13] A. Rusczyk, "New predictive algorithms of AC/DC and DC/AC inverters current control", *Ph.D. Thesis*, Technical University of Białystok Press, Białystok, 2005, (in Polish).